IEEE Photonics Journal
An IEEE Photonics Society Publication

Open Access

An Optically Coupled Electro-Optic Chaos System With Suppressed Time-Delay Signature

Volume 9, Number 3, June 2017

Xinhua Zhu
Mengfan Cheng
Lei Deng
XingXing Jiang
Changjian Ke
Minming Zhang
Songnian Fu
Ming Tang
Ping Shum
Deming Liu

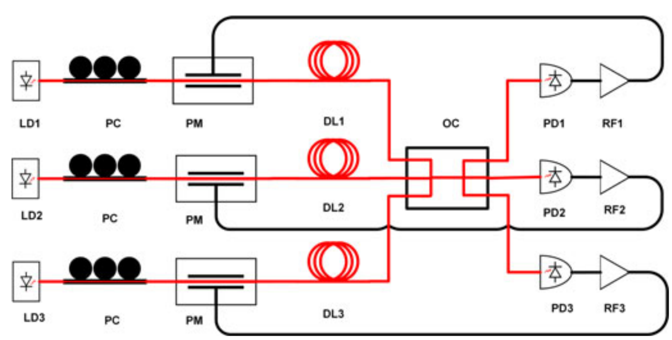

DOI: 10.1109/JPHOT.2017.2703899
1943-0655 © 2017 IEEE

An Optically Coupled Electro-Optic Chaos System With Suppressed Time-Delay Signature

Xinhua Zhu,[1] Mengfan Cheng,[1] Lei Deng,[1] XingXing Jiang,[1] Changjian Ke,[1] Minming Zhang,[1] Songnian Fu,[1] Ming Tang,[1] Ping Shum,[2] and Deming Liu[1]

[1]Next Generation Internet Access National Engineering Laboratory (NGIA), School of Optical and Electronic Information, Huazhong University of Science and Technology (HUST), Wuhan 430074, China
[2]School of Electrical and Electronic Engineering, College of Engineering, Nanyang Technological University (NTU), Singapore 639798

DOI:10.1109/JPHOT.2017.2703899

Manuscript received February 28, 2017; revised May 5, 2017; accepted May 9, 2017. Date of publication May 12, 2017; date of current version May 31, 2017. This work was supported the National Natural Science Foundation of China (NSFC) under Project no. 61505061 and 61675083, the National 863 Program of China under project no. 2015AA016904. Corresponding author: Mengfan Cheng (e-mail: chengmf@mail.hust.edu.cn).

Abstract: We present an optically coupled chaotic system involving three-phase modulated electro-optic nonlinear loops and an optical coupler. The dynamical properties and the time delay signature (TDS) suppressing performance of the system is analyzed in detail. Numerical results show that the TDS can be suppressed not only under statistical analysis of a single output, but also under mutual statistical analysis of the multiple outputs. Compared with the intensity modulated electrically coupled scheme, the presented system has less interior noise due to the simpler construction.

Index Terms: Optical chaos, time delay signature (TDS) suppression, electro-optic nonlinear loop.

1. Introduction

Chaotic dynamics of optical system have drawn considerable attention due to their advantages. With the broad bandwidth, large transmission capability and high level of privacy [1]–[5], the optical chaotic system has vast applications in fields such as secure communication [6]–[8], chaotic radar [9], [10] and fast physical random bit generation [11], [12]. Methods with external cavity and feedback loops can provide high-dimensional chaotic signals, which contain time delay signature (TDS) caused by the introduced periodic components. From the perspective of security, the attacker could reconstruct the chaotic carrier with the information of the TDS, and the dimension of the key space could be reduced [13], [14]. For random bit generation, the TDS will also impose restriction on the choices of sampling periods and limit the statistical performance [15]. These facts reveal the truth that the TDS is a vital key for these applications.

However, the TDS can be identified by using statistical methods including the autocorrelation function (ACF) [16], delayed mutual information (DMI) [17], the neural network and the filling factor analysis [18], [19], etc. Therefore, a series of effective schemes have been proposed for the purpose of concealing the TDS. Modified feedback approaches like distributed time delay feedback by using a fiber grating [20] and polarization-resolved chaos system [21] have been proposed. In [22]–[24], the TDS are eliminated in chaos communication systems by performing a digital phase mask, meanwhile the key space is significantly enlarged. System coupling is another type of effective way to deal with the problem of TDS. In [25], [26], electrical or optical heterodyne are adopted as the coupling strategy between two separated systems. In [27], the nonlinear dynamics in mutually coupled semiconductor lasers is investigated. In [28], [29], an electrically coupled chaos system with three nonlinear feedback loops is demonstrated. These coupled chaos systems can generate multiple TDS free chaos signals simultaneously, which could be used to improve the efficiency of chaotic radar [30] and secure communications under WDM scenario [29]. In these schemes, the TDS cannot be recovered through different statistical analyses under certain parameter range. However, the TDS analyses in the literatures are focused on the statistical feature of one single output, the mutual statistical feature between different signals is ignored. Unfortunately, the TDS can still be extracted by performing statistical analysis between the multiple outputs.

In this paper, an optically coupled chaotic system is proposed. It involves with three phase modulated electro-optic nonlinear loops and an optical coupler (OC). Not only can the TDS be concealed by the system itself under ACF and DMI analyses, but also it cannot be recovered by using mutual statistical methods to analyze two signals from different chains, either. Compared with our former proposed scheme [28], the proposed system has better performance and the system construction is much simpler.

2. System Model

The configuration of the optically coupled electro-optic chaos system is illustrated in Fig. 1. The system consists of three mutually coupled nonlinear chains. In each chain, the output of a continuous-wave laser diode (LD) is firstly modulated by a phase modulator (PM), which is used as an external nonlinear component, then detected by a photodetector (PD) and amplified by a radio-frequency (RF) driver. The polarization controller (PC) is used to achieve maximum modulation depth. The transfer function of PM is $E_{out} = E_{in}\, exp(j\pi V(t)/V_\pi)$, V_π means the half-wave voltage of PM. And the transfer function of PD is $V_{PD} = g \cdot |E(t) \cdot E^*(t)|$, g is the conversion gain. The transfer function of RF drivers is $V_{out} = G \cdot V_{in}$, where the constant G denotes the gain. The time delays introduced by the optical fibers are expressed as $DL_{i=1,2,3}$, and the latency of the other components is ignored. A 3×3 OC is adopted to make the three chains couple to each other in optical field.

Ordinarily, a phase-modulation to intensity-modulation converter (like a Mach–Zehnder interferometer [22] or an optical filter [31]) is indispensable in phase chaos system. In our system, such conversion is realized by an OC, which achieves the interferences between the three different chains. Meanwhile the coupling is conducted in this process. Compared with our former proposed intensity coupled scheme in [28], the advantages on system structure lie in two aspects. Firstly, phase modulating avoids the bias controlling which is necessary in intensity modulating. Secondly, an OC takes place of multiple electrical power splitters and electrical power combiners. As a result, the system structure is simpler, and the stability of the system could be better due to the fact that the introduced noise in an OC is much smaller than that in multiple electrical components.

The mathematical model of the system can be derived as follows. The coupling matrix of the 3×3 OC is expressed as:

$$\begin{bmatrix} E_1' \\ E_2' \\ E_3' \end{bmatrix} = e^{-jpz} \begin{bmatrix} f & c & c \\ c & f & c \\ c & c & f \end{bmatrix} \begin{bmatrix} E_1 \\ E_2 \\ E_3 \end{bmatrix} \tag{1}$$

where k, z and p mean coupling factor, coupling length and propagation constant of the OC respectively. And

$$f = [\exp(i2kz) + 2exp(-ikz)]/3,$$

$$c = [\exp(i2kz) - 2exp(-ikz)]/3.$$

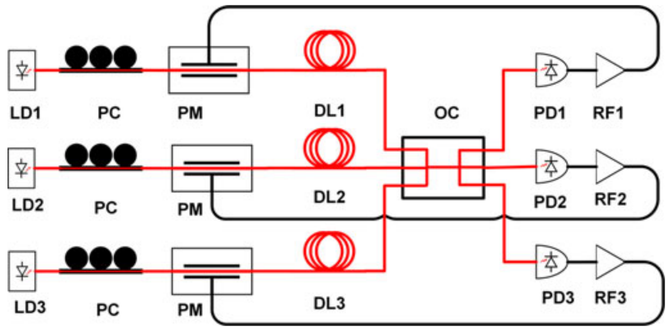

Fig. 1. The configuration of the optically coupled electro-optic chaos system.

In (1), $E_i = E_{i0}\ exp\ (j(w_i t - x_i(t))) = E_{i0}\ exp(j(w_i t - \pi V_i(t)/2V_\pi))$ means the electric field of the transmitted signal after PM. $x_i\ (t) = \pi V_i(t)/2V_\pi$ represents the dimensionless variable describing the system. $V_i(t)$ is the electrical voltage for PM electrode. E_i', $i = 1, 2, 3$ means the electric field after OC. Then we get:

$$\begin{bmatrix} E_1' \\ E_2' \\ E_3' \end{bmatrix} = n \begin{bmatrix} 1 & m & m \\ m & 1 & m \\ m & m & 1 \end{bmatrix} \begin{bmatrix} E_{10} \exp(\mathrm{j}(w_1 \mathrm{t} - x_1(\mathrm{t}))) \\ E_{20} \exp(\mathrm{j}(w_2 \mathrm{t} - x_2(\mathrm{t}))) \\ E_{30} \exp(\mathrm{j}(w_3 \mathrm{t} - x_3(\mathrm{t}))) \end{bmatrix} \tag{2}$$

where $m = \frac{e^{3jkz}-1}{e^{3jkz}+2}$, $n = \frac{e^{-j(k+p)z}(e^{3jkz}+2)}{3}$, when $kz = 2\pi/9$, $|\mathrm{m}| = 1$. The input power of the coupler is separated to the three output chains homogeneously. Suppose the frequencies of the three LDs as f_0, $f_0 + \Delta f$, $f_0 + 2\Delta f$, Δf means the frequency detuning. When the frequency detuning $\Delta f = 0$, the three lasers have same wavelength. The dynamical equation of the coupled chaotic system can be described as:

$$\begin{aligned} & x_1 + \tau_1 \frac{dx_1}{dt} + \frac{1}{\theta_1}\int_0^t (x_1(s)ds) = \beta_1 \frac{5 + cos3kz}{9} \\ & \cdot |exp(-jx_1(t)) + mexp(j(2\pi\Delta f - x_2(t))) + mexp(j(4\pi\Delta f - x_3(t)))|^2. \\ & x_2 + \tau_2 \frac{dx_2}{dt} + \frac{1}{\theta_2}\int_0^t (x_2(s)ds) = \beta_2 \frac{5 + cos3kz}{9} \\ & \cdot |mexp(-jx_1(t)) + exp(j(2\pi\Delta f - x_2(t))) + mexp(j(4\pi\Delta f - x_3(t)))|^2. \\ & x_3 + \tau_3 \frac{dx_3}{dt} + \frac{1}{\theta_3}\int_0^t (x_3(s)ds) = \beta_3 \frac{5 + cos3kz}{9} \\ & \cdot |mexp(-jx_1(t)) + mexp(j(2\pi\Delta f - x_2(t))) + exp(j(4\pi\Delta f - x_3(t)))|^2. \end{aligned} \tag{3}$$

In (3), $\beta_i = \beta = \pi gAGP/2V_\pi$ is defined as the loop gain, which is also considered as the bifurcate parameter, where A means the overall attenuation of this feedback loop, P means the output power of the LD. The bandwidth of the feedback loop is supposed in first approximation to result from a bandpass filter, with low and high cutoff frequencies f_L and f_H, respectively, where $\theta = 1/2\pi f_L$, $\tau = 1/2\pi f_H$. Parameters in the system are: $\tau_i = \tau = 25$ ps and $\theta_i = \theta = 5$ us. The time delay in the three chains are set as $T_i = 30$, 25 and 20 ns respectively, $i = 1, 2, 3$.

The simulations in our work are conducted by using the MATLAB tool. Equation (3) is calculated with a fourth-order Runge-Kutta algorithm. The variable-step is 1/60ns. Fig. 2(a)–(c) show the time series while $\beta = 0.7, 1.0, 3$ respectively. When $\beta < 0.6$, the oscillation is hard to start due to the small loop gain, so the output attenuates to zero. While β is about 0.7, the electrical input of PM is small and the transfer function of PM can be treated as linear approximately. The feedback loop can be seen as a linear oscillator, and the output is periodic. When β increases, the nonlinearity

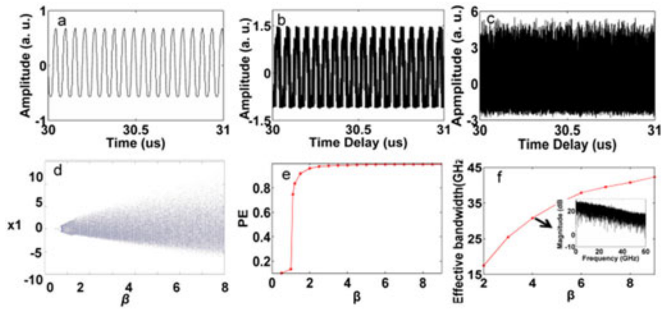

Fig. 2. (a) Time series while $\beta = 0.7$; (b) time series while $\beta = 1.0$; (c) time series while $\beta = 3$; (d)Bifurcation diagram of system; (e) PE as a function of β for the ordinal pattern length $L = 6$ and the embedding delay $D = 2$; (f) effective bandwidth of the transmitted signal as a function of β, the insets shows the spectrum of the transmitted signal with $\beta = 4$;

of the loop is emerging, quasi-periodic oscillation can be observed. Continuing to increase β, the system evolves into chaotic state due to the strong nonlinearity of the loop. These process can also be observed in the bifurcation diagram, as shown in Fig. 2(d). Permutation entropy (PE) [32] is used to map the dynamical complexity. We choose a time series x_1 with length of 4×10^4. PE is calculated for the ordinal pattern length $L = 6$ and the embedding delay $D = 2$. The embedding delay corresponds to the sampling time of the signal. The time series is partitioned into subsets of ordinal pattern length with embedding delay. Result is shown in Fig. 2(e). The curve of PE shows that the system can generate the most complex time series (PE = 0.99) in the chaotic zone.

The spectrum characteristic of the optical chaos signal is also analyzed. Due to the drastic fluctuations in the spectrum, the bandwidth may not be very easy to estimate by using the concept of "3 dB bandwidth". Here we use the principle of effective bandwidth [33]. The signal energy is calculated from 0 to 60 GHZ. The effective bandwidths of the generated optical chaos signals are demonstrated in Fig. 2(f) while β ranges from 2 to 9. Since the numerical value of the effective bandwidth relies on the calculating range, this result is only used to demonstrate a qualitative relationship between β and the spectrum. The complexity and the bandwidth performance of the presented system are similar to the intensity coupled chaotic system. In real world applications, β should be as large as possible for large bandwidth and high dynamical complexity, but the value of β is restricted by the half wave voltage of the modulator and the gain of the RF driver.

3. Main Results

3.1 Statistical Analysis With Single Time Series

In this work, we discuss the concealment of the TDS, which plays an important role in chaos-based applications. We define $T = (T_1, T_2, T_3)$, and time delay difference $\Delta T = T_1 - T_2 = T_2 - T_3$. Time series x_1 with length of 10^6 (from 1×10^6 to 2×10^6) are used to perform ACF and $\mathrm{DMI_s}$ (which means DMI analysis of a single output)analysis for $T = (25, 25, 25)$ns, $T = (27, 25, 23)$ns and $T = (30, 25, 20)$ns. The formula of ACF(v) and $\mathrm{DMI_s}(v)$ for a single time series $v(t)$ can be expressed as

$$C_s(\Delta t) = \frac{\langle (v(t+\Delta t) - \langle v(t)\rangle)\,(v(t) - \langle v(t)\rangle)\rangle}{\left(\langle v(t) - \langle v(t)\rangle\rangle^2 \langle v(t+\Delta t) - \langle v(t)\rangle\rangle^2\right)^{1/2}} \tag{4}$$

$$I_s(\Delta t) = \sum p\,(v(t), v(t+\Delta t))\, ln \frac{p\,(v(t), v(t+\Delta t))}{p\,(v(t))\, p\,(v(t+\Delta t))} \tag{5}$$

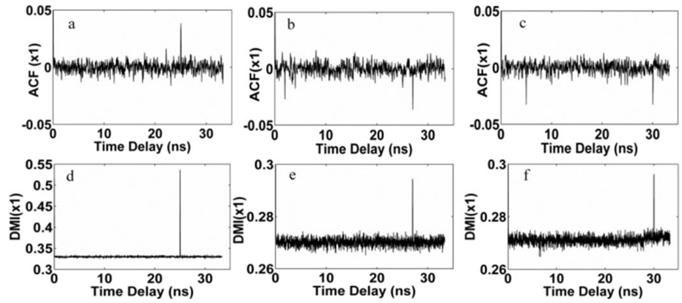

Fig. 3. ACF(x_1) and DMI$_s$ (x_1)curve while the parameter is given as $\beta = 4$. (a) ACF(x_1) while $T = (25, 25, 25)$ns; (b) ACF(x_1) while $T = (27, 25, 23)$ns; (c) ACF(x_1) while $T = (30, 25, 20)$ns; (d) DMI$_s$ (x_1) while $T = (25, 25, 25)$ns; (e) DMI$_s$ (x_1)while $T = (27, 25, 23)$ns; (f) DMI$_s$ (x_1) while $T = (30, 25, 20)$ns.

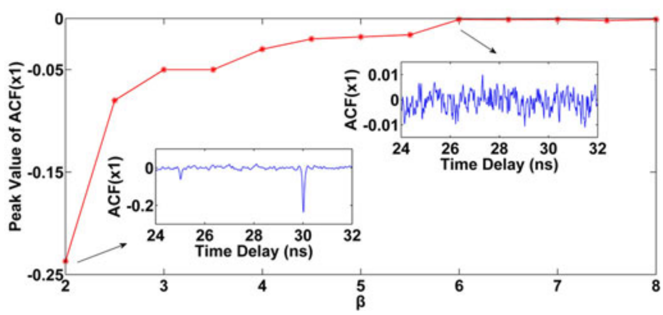

Fig. 4. Value of the peaks at $T = 30$ ns in ACF (x_1). The insets shows the ACF (x_1) curves while $\beta = 2$ and 6.

where $v(t)$ represents single chaotic time series x_1, Δt means the time shift. $\langle\cdot\rangle$ means time average. $p(v(t))$ and $p(v(t), v(t + \Delta t))$ are mean probability distribution of marginal and joint fault probability distribution respectively. The results of ACF(x_1) and the DMI$_s$ (x_1) while $\beta = 4$ are shown in Fig. 3.

As it can be seen, clear peaks appeared at time shift T_1, which reveal the TDS. When ΔT increases, the peak values in ACF(x_1) barely have no change. But the peak values in DMI$_s$ (x_1) decrease while ΔT increases from 0 to 5ns; Continue to increase ΔT, the peak values in DMI$_s$ (x_1) remain static. So in the following parts, the time delay in three chains are chosen as $T = (30, 25, 20)$ ns.

The influence of the bifurcate parameter β on the TDS concealment is also discussed in detail. ACF and DMI$_s$ analyses have been conducted while β ranges from 2 to 8. As it can been seen in Fig. 4, which displays the peak value at $T = 30$ ns from the background in ACF(x_1), the peak is distinguishable for $\beta = 2.5\sim3.5$; When β increases to 4.5, the peak becomes unobvious; And when β continues to rise to a critical large value like $\beta = 6$, the peak is entirely buried in the background. Similar phenomena can be observed in the results of DMI$_s$ (x_1), as shown in Fig. 5. Therefore, the TDS will be concealed successfully in ACF (x_1) and DMI$_s$ (x_1) while $\beta > 6$. It is also suitable for time series x_2 and x_3 due to the symmetry of the system structure.

3.2 Mutual Statistical Analysis With Two Different Time Series

According to the system setup and theoretical model, three sets of chaotic signal transmitted in separate chains can be obtained. The aforementioned results show that the TDS can be eliminated under statistical analysis based on one single time series. However, for coupled systems, the mutual statistical feature between different sub-systems could cause the information leak. It was proposed in [34] that cross correction function (CCF) could be used to analyze TDS of the rings of

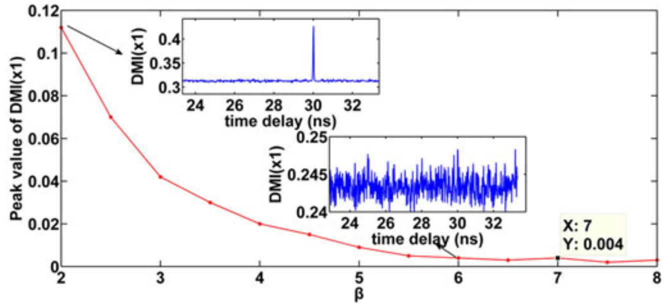

Fig. 5. Value of the peaks at $T = 30$ ns in DMI (x_1). The insets show the $\mathrm{DMI_s}$ (x_1) curves while $\beta = 2$ and 6.

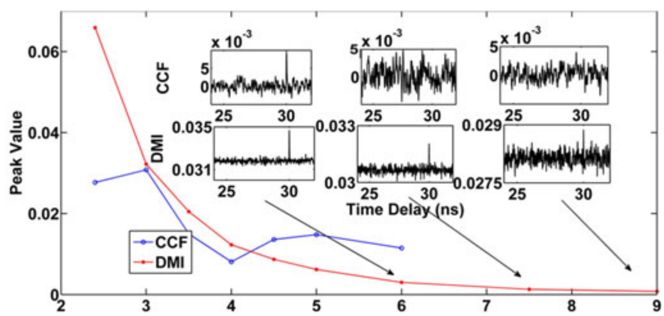

Fig. 6. The peak values of the CCF(x_1, x_2) and $\mathrm{DMI_d}$ (x_1, x_2) curves of the electrically coupled electro-optic chaos system while β ranges from 2 to 9. The insets show the CCF and DMI curves while $\beta = 6$, 7.5 and 9.

delay-coupled elements. In this paper, mutual statistical methods CCF and $\mathrm{DMI_d}$ (which means DMI analysis of double outputs)are performed between double outputs of different chains. The formula of CCF(v_1, v_2) and $\mathrm{DMI_d}$(v_1, v_2) for two different time series $v_1(t)$ and $v_2(t)$ can be expressed as:

$$C_d(\Delta t) = \frac{\langle (v_1(t) - \langle v_1(t)\rangle)\,(v_2(t+\Delta t) - \langle v_2(t)\rangle)\rangle}{\left(\langle v_1(t) - \langle v_1(t)\rangle\rangle^2 \langle v_2(t+\Delta t) - \langle v_2(t)\rangle\rangle^2\right)^{1/2}} \tag{6}$$

$$I_d(\Delta t) = \sum p\,(v_1(t), v_2(t+\Delta t))\, ln \frac{p\,(v_1(t), v_2(t+\Delta t))}{p\,(v_1(t))\,p\,(v_2(t+\Delta t))}. \tag{7}$$

First, we consider our former scheme, the electrically coupled electro-optic chaos system. According to [28], we can conclude that the TDS will be concealed in ACF (x_1) and $\mathrm{DMI_s}$ (x_1) if the bifurcate parameter $\beta > 4$ under single time series analysis. However, the statistical property between two time series x_1 and x_2 can be revealed by CCF (x_1, x_2) and $\mathrm{DMI_d}$ (x_1, x_2). As shown in Fig. 6, the peak values of CCF (x_1, x_2) and $\mathrm{DMI_d}$ (x_1, x_2) exist while $\beta > 4$, the peaks are apparent though the absolute value decreases if we increase β. When $\beta = 6$, the TDS can still be extracted under $\mathrm{DMI_d}$ (x_1, x_2). These results indicate that the electrically coupled electro-optic chaotic system is not safe enough under mutual statistical analysis.

In the same way, CCF (x_1, x_2) and $\mathrm{DMI_d}$ (x_1, x_2) are used to analyze the system presented in this article. As shown in Fig. 7, the peaks in CCF and $\mathrm{DMI_d}$ are both entirely buried in the background when $\beta = 6$, which means that the TDS cannot be revealed even under mutual analysis.

3.3 The Influence of Frequency Detuning

The three nonlinear loops are coupled in optical field by an OC. This fact makes the wavelength of the light source a new degree of freedom to investigate the system. The frequency detuning between

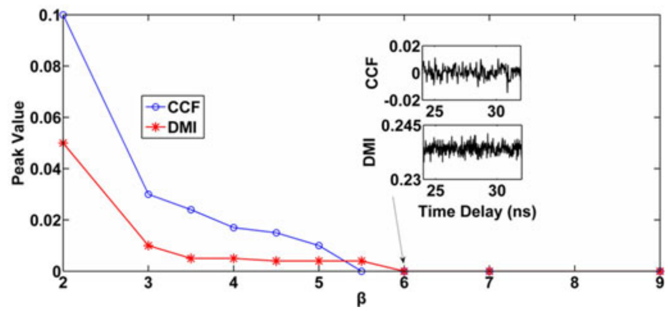

Fig. 7. The peak values of the CCF (x_1, x_2) and DMI$_d$ (x_1, x_2) curves of the presented system while β ranges from 2 to 9. The insets show the CCF and DMI curves while $\beta = 6$ and 7.

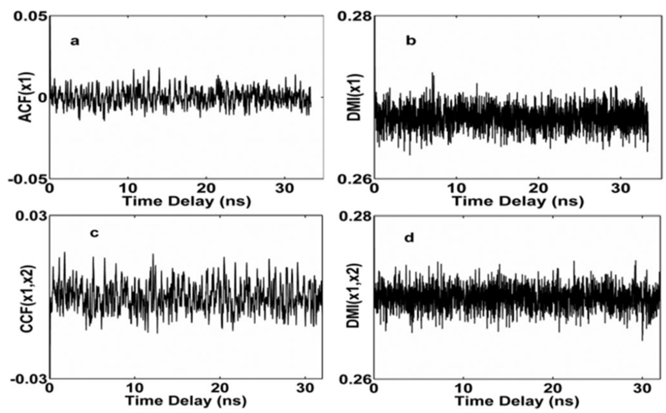

Fig. 8. The ACF(x_1), DMI$_s$ (x_1)and CCF(x_1, x_2), DMI$_d$ (x_1, x_2) curves while $\Delta f = 1$ Ghz, $\beta = 4$. (a) ACF(x_1); (b) DMI$_s$ (x_1); (c) CCF(x_1, x_2); (d) DMI$_d$ (x_1, x_2).

the optical sources could affect the performance of the chaotic system. When $\Delta f = 1$ GHz, the single chain analysis of the transmitted signal x_1 are shown in Fig. 8(a) and (b). The mutual property between the different chains is also analyzed by CCF (x_1, x_2) and DMI$_d$ (x_1, x_2), which are shown in Fig. 8(c) and (d). These results indicate that the TDS are concealed under ACF and DMI$_s$ analysis and the system can also resist the CCF and DMI$_d$ attack with two signals in the different chains.

Similar conclusions can be obtained while the frequency detuning ranges from 0.5 to 15 GHz, the TDS are totally suppressed while $\beta > 4$. Compared with the results in Figs. 4–6, the frequency detuning between the optical sources play a positive role in TDS suppression. Smaller β is needed to achieve the TDS suppression, which means the system is easier to implement. Considering that large β has a high demand for the half-wave voltage of PM and the gain of the RF, the presented system has advantages in the implementation cost and the performance of TDS suppression.

In real world systems, even with the same wavelength, the lasers will have phase noise due to a finite linewidth. We have analyzed the performance of the TDS suppression when the lasers in our model have typical linewidth like 100 KHz–1 MHz. Similar results could be obtained and no significant influence is observed. Those mean that the laser linewidth has few influences on the performance of TDS suppression. The reason could be attributed to the fact that the beat interference caused by the phase noise is limited in low frequency region of a few hundred kHz or several MHz. However, the generated chaotic signals are broadband signals. The energy is distributed in a wide frequency range of several GHz. As a result, the low frequency noise will not affect the system performance significantly.

4. Conclusion

In summary, we have present an optically coupled chaotic system based on electro-optic loops and OC. The OC introduces interference between the different loops of chaotic dynamics. We have investigated the performances of the chaotic dynamic and analyses the statistical properties of the system. The results show that the TDS information can't be recovered by ACF, DMI_s analysis of one single output under proper range. And the system can also resist mutual statistical analysis like CCF and DMI_d between multiple outputs. With the introducing of frequency detuning, the proposed system can conceal the TDS by itself in a larger range. What's more, the system has less interior noise than the intensity modulated electrically coupled scheme due to the introducing of the phase modulator and the OC. The presented system has advantage in the implementation cost and the performance of the TDS suppression, which make the presented system gain a promising expectation in secure communications and fast physical random number generation in the future.

References

[1] R. M. Nguimdo and P. Colet, "Electro-optic phase chaos systems with an internal variable and a digital key," *Opt. Exp.*, vol. 20, no. 23, pp. 25333–25344, 2012.
[2] Y. Hong, W. L. Min, J. Paul, and P. S. Spencer, "Ghz bandwidth message transmission using chaotic vertical-cavity surface-emitting lasers," *J. Lightw. Technol.,* vol. 27, no. 22, pp. 5099–5105, Nov. 15, 2009.
[3] A. Argyris *et al.*, "Chaos-based communications at high bit rates using commercial fibre-optic links," *Nature*, vol. 438, pp. 343–346, 2005.
[4] S. Wieczorek and W. W. Chow, "Bifurcations and chaos in a semiconductor laser with coherent or noisy optical injection," *Opt. Commun.*, vol. 282, pp. 2367–2379, 2009.
[5] Y. H. Liao, J. M. Liu, and F. Y. Lin, "Dynamical characteristics of a dual-beam optically injected semiconductor laser," *IEEE J. Sel. Topics Quantum Electron.*, vol. 19, Jul./Aug. 2013, Art. no. 1500606.
[6] V. Annovazzi-Lodi, G. Aromataris, and M. Benedetti, "Multi-user private transmission with chaotic lasers," *IEEE J. Quantum Electron*, vol. 48, no. 8, pp. 1095–1101, Aug. 2012.
[7] N. Jiang *et al.*, "Chaos synchronization and communication in mutually coupled semiconductor lasers driven by a third laser," *J. Lightw. Technol.,* vol. 28, no. 13, pp. 1978–1986, Jul. 1, 2010.
[8] C. R. Mirasso, J. Mulet, and C. Masoller, "Chaos shift-keying encryption in chaotic external-cavity semiconductor lasers using a single-receiver scheme," *IEEE Photon. Technol. Lett.*, vol. 14, no. 4, pp. 456–458, Apr. 2002.
[9] F. Y. Lin and J. M. Liu, "Chaotic radar using nonlinear laser dynamics," *IEEE J. Quantum Electron.,* vol. 40, no. 6, pp. 815–820, Jun. 2004.
[10] W. T. Wu, Y. H. Liao, and F. Y. Lin, "Noise suppressions in synchronized chaos lidars," *Opt. Exp.,* vol. 18, pp. 26155–26162, 2010.
[11] A. Uchida, *et al.*, "Fast physical random bit generation with chaotic semiconductor lasers," *Nat. Photon.,* vol. 2, pp. 728–732, 2008.
[12] T. Butler *et al.*, "Optical ultrafast random number generation at 1 tb/s using a turbulent semiconductor ring cavity laser," *Opt. Lett.,* vol. 41, pp. 388–391, 2016.
[13] M. C. Soriano, P. Colet, and C. R. Mirasso, "Security implications of open- and closed-loop receivers in all-optical chaos-based communications," *IEEE Photon. Technol. Lett.,* vol. 21, no. 7, pp. 426–428, Apr. 1, 2009.
[14] L. Ursini, M. Santagiustina, and V. Annovazzi-Lodi, "Enhancing chaotic communication performances by Manchester coding," *IEEE Photon. Technol. Lett.,* vol. 20, no. 6, pp. 401–403, Mar. 15, 2008.
[15] I. Reidler, Y. Aviad, M. Rosenbluh, and I. Kanter, "Ultrahigh-speed random number generation based on a chaotic semiconductor laser," *Phys. Rev. Lett.,* vol. 103, pp. 024102–024105, 2009.
[16] V. S. Udaltsov *et al.*, "Cracking chaos-based encryption systems ruled by nonlinear time delay differential equations," *Phys. Lett. A*, vol. 308, pp. 54–60, 2003.
[17] V. S. Udaltsov, L. Larger, J. P. Goedgebuer, A. Locquet, and D. S. Citrin, "Time delay identification in chaotic cryptosystems ruled by delay-differential equations," *J. Opt. Technol. C/c Opticheskii Zhurnal*, vol. 72, pp. 373–377, 2005.
[18] M. D. Prokhorov, V. I. Ponomarenko, A. S. Karavaev, and B. P. Bezruchko, "Reconstruction of time-delayed feedback systems from time series," *Phys. D, Nonlinear Phenomena*, vol. 203, pp. 209–223, 2005.
[19] S. Ortín, J. M. Gutiérrez, L. Pesquera, and H. Vasquez, "Nonlinear dynamics extraction for time-delay systems using modular neural networks synchronization and prediction," *Phys. A Statistical Mech. Appl.,* vol. 351, pp. 133–141, 2005.
[20] S. S. Li, Q. Liu, and S. C. Chan, "Distributed feedbacks for time-delay signature suppression of chaos generated from a semiconductor laser," *IEEE Photon. J.,* vol. 4, no. 5, pp. 1930–1935, Oct. 2012.
[21] P. Xiao *et al.*, "Time-delay signature concealment of chaotic output in a vertical-cavity surface-emitting laser with double variable-polarization optical feedback," *Opt. Commun.,* vol. 286, pp. 339–343, 2013.
[22] R. M. Nguimdo, P. Colet, L. Larger, and L. Pesquera, "Digital key for chaos communication performing time delay concealment," *Phys. Rev. Lett.,* vol. 107, p. 034103, 2011.
[23] C. Xue *et al.*, "Security-enhanced chaos communication with time-delay signature suppression and phase encryption," *Opt. Lett.,* vol. 41, no. 16, p. 3690, 2016.
[24] M. Cheng, L. Deng, H. Li, and D. Liu, "Enhanced secure strategy for electro-optic chaotic systems with delayed dynamics by using fractional Fourier transformation," *Opt. Exp.,* vol. 22, no. 5, pp. 5241–5251, 2014.

[25] C. H. Cheng, Y. C. Chen, and F. Y. Lin, “Chaos time delay signature suppression and bandwidth enhancement by electrical heterodyning,” *Opt. Exp.,* vol. 23, pp. 2308–2319, 2015.
[26] A. Wang, B. Wang, L. Li, Y. Wang, and K. A. Shore, “Optical heterodyne generation of high-dimensional and broadband white chaos,” *IEEE J. Sel. Topics Quantum Electron*, vol. 21, no. 6, pp. 1–10, Nov./Dec. 2015.
[27] J. G. Wu, Z. M. Wu, G. Q. Xia, and G. Y. Feng, “Evolution of time delay signature of chaos generated in a mutually delay-coupled semiconductor lasers system,” *Opt. Exp.,* vol. 20, pp. 1741–1753 2012.
[28] M. Cheng *et al.*, “Time-delay concealment in a three-dimensional electro-optic chaos system,” *IEEE Photon. Technol. Lett.,* vol. 27, no. 9, pp. 1030–1033, May 1, 2015.
[29] X. Gao *et al.*, “A novel chaotic system with suppressed time delay signature based on multiple electro-optic nonlinear loops,” *Nonlinear Dyn.,* vol. 82, pp. 611–617, 2015.
[30] M. Zhang *et al.*, “Remote radar based on chaos generation and radio over fiber,” *IEEE Photonics J.,* vol. 6, no. 5, pp. 1–12, Oct. 2014.
[31] B. Romeira *et al.*, “Broadband chaotic signals and breather oscillations in an optoelectronic oscillator incorporating a microwave photonic filter,” *J. Lightwave Technol.,* vol. 32, no. 20, pp. 3933–3942, Oct. 15, 2014.
[32] C. Bandt and B. Pompe, “Permutation entropy: A natural complexity measure for time series,” *Phys. Rev. Lett.,* vol. 88, p. 174102, 2002.
[33] F. Y. Lin and J. M. Liu, “Nonlinear dynamical characteristics of an optically injected semiconductor laser subject to optoelectronic feedback,” *Opt. Commun.,* vol. 221, no. 1–3, pp. 173–180, 2003.
[34] O. D’Huys, I. Fischer, J. Danckaert, and R. Vicente, “Spectral and correlation properties of rings of delay-coupled elements: Comparing linear and nonlinear systems,” *Phys. Rev. E*, vol. 85, pp. 1413–1413, 2012.